CORRELATED IRON AND SILICON ISOTOPE COMPOSITIONS OF AUBRITES AS TRACERS OF DIFFERENTIATION PROCESSES.

S. Ray and M. Wadhwa, School of Earth and Space Exploration, Arizona State University, Tempe, AZ- 85287 (soumya.ray@asu.edu).

Introduction: The formation of a core is a fundamental physical and chemical process in the evolutionary history of a rocky planet. Mass transfer of Fe and other alloying elements during core formation is expected to induce isotopic fractionation between the metallic core and silicate mantle. The magnitude of the isotopic fractionation of a particular element is dependent on the bonding environment of that element such that a stronger bond will favor the enrichment of heavier isotopes in comparison to a weaker bond [1, 2]. In the case of Fe and Si isotopes, several studies have attempted to constrain the magnitude of isotopic fractionation due to core formation through the investigation of meteorites [3-11], laboratory experiments [12-19], first principles-based calculations [8,13], and Nuclear Resonant Inelastic X-Ray spectroscopy [20-22].

According to the first principles of crystal-chemistry involving bond strength, Fe-metal will be enriched in the heavier isotopes of Fe [1, 2] rendering co-existing silicates with a lighter Fe isotopic composition, i.e., $\delta^{56}Fe_{metal} > \delta^{56}Fe_{silicate}$ where δ^{56}Fe is the parts per thousand deviation in the ^{56}Fe/^{54}Fe ratio relative to the IRMM-014 bracketing standard. Similarly, when Si alloys with Fe-metal (as a result of increasing pressure, temperature, or decreasing fO_2 [23]), the Fe-metal will be enriched in the lighter isotopes of Si compared to the silicates [2], i.e., $\delta^{30}Si_{metal} < \delta^{30}Si_{silicate}$ where δ^{30}Si is the parts per thousand deviation in the ^{30}Si/^{28}Si ratio relative to the NBS-28 bracketing standard. Hence, in a differentiated body that would sequester Si in its metallic core, the core is expected to have heavier δ^{56}Fe and lighter δ^{30}Si compared to its bulk starting composition while the silicate mantle is expected to be characterized by a complementary lighter δ^{56}Fe and heavier δ^{30}Si.

Aubrites are ortho-pyroxenites that have Si-bearing metal co-existing with silicates and sulfides [24] and are considered to be differentiated products of an enstatite chondrite-like precursor [25,26]. Here, we demonstrate that incorporation of Si into the core of the aubrite parent body can indeed explain both the δ^{56}Fe and δ^{30}Si composition of aubrites. This work is part of an ongoing effort to determine the δ^{56}Fe and δ^{30}Si compositions in a single sample aliquot of a variety of meteorites [27] to assess the role of core formation and partial melting in such isotopic fractionation and whether δ^{30}Si–δ^{56}Fe compositions can be used as tracers of planetary differentiation.

Method and Results: Assuming that the aubrites originated as the silicate portion of a differentiated body that was initially EH chondrite-like in composition, the fraction of total Si that goes into the core of the aubrite parent body (f_{Si}^{core}) can be calculated based on the difference in the Si isotope compositions of the aubrites and the EH chondrites using the following mass balance equation,

$$\delta^{30}Si_{aubrites} - \delta^{30}Si_{EH} = f_{Si}^{core}(\Delta^{30}Si_{silicate-metal}) \quad (1)$$

where $\Delta^{30}Si_{silicate-metal}$ is $\frac{7.64\times10^{6}}{T^{2}}$ [9] and T is the peak temperature attained in the aubrite parent body [28]. The fraction of total Si in the core thus calculated (i.e., f_{Si}^{core}= 0.025), yields the concentration of Si in the core (C_{Si}^{core}~ 2.1 wt %) using the following equation,

$$f_{M}^{core} = \left[1 + \left(\frac{C_{M}^{mantle}}{C_{M}^{core}}\right) \times \left(\frac{M_{mantle}}{M_{core}}\right)\right]^{-1} \quad (2)$$

where $C_{M}^{reservoir}$ is the mass fraction of solute M (in this case Si) in that reservoir (i.e., mantle or core), M_{mantle} and M_{core} are the masses of mantle and core of the aubrite parent body [29]. The value obtained for C_{Si}^{core} (i.e., 2.1 wt.%) is similar to that of the aubrite metals that equilibrated at the peak temperature attained in the aubrite parent body [28]. Thereafter, based on the average elemental composition of aubrite metals that equilibrated at the peak temperature [28] and the Fe isotope equilibration factor $\Delta^{56}Fe_{metal-silicate}$= $\frac{3.85\times10^{4}(X_{sub})+7.44\times10^{4}}{T^{2}}$ [19], the $\delta^{56}Fe_{mantle}$ of the aubrite parent body is calculated to be −0.160±0.066‰ using the following mass balance equation,

$$\delta^{56}Fe_{mantle} = \delta^{56}Fe_{EH} - f_{Fe}^{core}(\Delta^{56}Fe_{metal-silicate}) \quad (3)$$

To account for the effect of 'missing' enstatite-plagioclase basalts [30] on the $\delta^{56}Fe_{mantle}$ (calculated above) and $\delta^{56}Fe_{residue}$ (aubrites), we have used the following formula [31],

$$\delta^{56}Fe_{residue} - \delta^{56}Fe_{mantle} \approx -F(\Delta^{56}Fe_{melt-solid}) \quad (4)$$

where F is the degree of melting on the aubrite parent body which is 7−20% [28] and $\Delta^{56}Fe_{melt-solid}$= 0.053±0.017 in Fe^{3+}-free systems [18,19]. The $\delta^{56}Fe_{residue}$ is calculated to be −0.168‰±0.068‰ which overlaps with the δ^{56}Fe composition of main group aubrites [6]. Therefore, the δ^{30}Si–δ^{56}Fe composition of aubrites can be explained in terms of core formation and partial melting on the aubrite parent body.

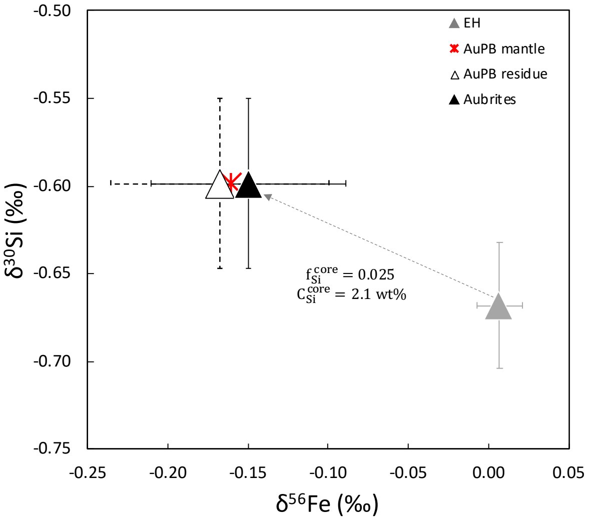

Figure 1: δ^{30}Si versus δ^{56}Fe in main group aubrites [6,32] and EH chondrites [6,8,10,32-36]. Assuming an EH chondrite-like starting composition, separation of a metallic core with f_{Si}^{core}=0.025 and subsequent partial melting will result in a residue that is consistent with the δ^{30}Si–δ^{56}Fe systematics of main group aubrites.

Discussion and Conclusions: The δ^{56}Fe and δ^{30}Si compositions of distinct planetary materials have been attributed to a variety of processes such as, nebular condensation [37,38], volatile depletion [3,39-43], core formation [8,9,13,14,17-19], and partial melting [5,31,44]. In particular, there have been many investigations of either Fe or Si isotope compositions (but not both together) in a variety of planetary materials as well in experimental run products to assess the effects of core formation in planetesimals and planetary bodies.

The difference in the δ^{56}Fe values between chondrites and magmatic iron meteorites could be due to the enrichment of heavy Fe isotopes in the metal during core formation on meteorite parent bodies [45]. However, the chondritic or heavier δ^{56}Fe values of samples from the silicate portions of differentiated bodies such as terrestrial mantle and basalts [31], lunar basalts [43], SNC meteorites from Mars, HED meteorites from Vesta, and angrites [46] have been interpreted as the lack of significant fractionation of Fe isotopes during core formation and instead attributed to volatilization processes [3,39-43]. On the contrary, results of metal-silicate equilibration experiments suggest that δ^{56}Fe values of terrestrial and lunar basalts, SNCs, and HEDs can be explained by core formation followed by partial melting on their respective parent bodies [18,19]. Similarly, the heavy δ^{30}Si of bulk silicate Earth compared to chondrites has been interpreted as the incorporation of lighter Si isotopes into Earth's core [8]. On the other hand, the heavy δ^{30}Si of angrites has been considered a result of nebular condensation [37] or volatile depletion [39] as the angrite parent body formed under relatively oxidizing conditions and did not have a Si-bearing core.

Both Fe as well as Si isotope compositions of differentiated meteorites can provide insights into differentiation processes such as core formation and silicate partial melting. As illustrated here, when used together, the combined Fe and Si isotope systematics can elucidate such differentiation processes on meteorite parent bodies. Nevertheless, coordinated studies of Fe and Si isotopes in the same aliquots of different types of differentiated planetary materials have yet to be conducted. Therefore, we have developed the analytical protocols for simultaneously conducting analyses of both Fe and Si isotope compositions in the same samples [27], and are in the process of conducting such analyses of a variety of achondritic meteorites.

Acknowledgments: This work was supported by a NASA Emerging Worlds grant (NNX15AH41G) to MW and NESSF grant (80NSSC18K1269) to SR and MW.

References: [1] Schauble E. A. (2004) *Reviews in Min. and Geochem., 55,* 65-111. [2] Young E. D. et al. (2015) *Chemical Geology, 395,* 176-195. [3] Poitrasson F. et al. (2004) *EPSL, 223,* 253-266. [4] Poitrasson F. et al. (2005) *EPSL, 234,* 151-164. [5] Weyer S. et al. (2005) *EPSL, 240,* 251-264. [6] Wang K. et al. (2014) *GCA, 142,* 149-165. [7] Jordan M. K. et al. (2019) *GCA, 246,* 461-477. [8] Georg R. B. et al. (2007) *Nature, 447,* 1102-1106. [9] Ziegler K. et al. (2010) *EPSL, 295,* 487-496. [10] Armytage R. M. G. et al. (2011) *GCA, 75,* 3662-3676.; [11] Moynier F. et al. (2020) *EPSL*, 549, 116468. [12] Poitrasson F. et al. (2009) *EPSL, 278,* 376-385. [13] Shahar A. et al. (2009) *EPSL, 288,* 228-234. [14] Shahar A. et al. (2011) *GCA, 75,* 7688-7697. [15] Hin R. C. et al. (2012) *GCA, 93,* 164-181. [16] Hin R. C. et al. (2014) *EPSL, 387,* 55-66. [17] Shahar A. et al. (2015) *GCA, 150,* 253-264. [18] Elardo S. M. and Shahar A. (2017) *Nature Geoscience, 10,* 317-321. [19] Elardo S. M. et al. (2019) *EPSL, 513,* 124-134. [20] Polyakov V. B. (2009) *Science, 323,* 912-914. [21] Shahar A. et al. (2016) Science, 352, 580-582. [22] Liu J. et al. (2017) *Nat. Commun.*, *8,* 14377. [23] Gessmann C. K. et al. (2001) *EPSL, 184,* 367-376. [24] Keil K. (2010) *Chemie der Erde, 70,* 295–317. [25] Casanova I. et al. (1993) *GCA, 57,* 675-682. [26] Lodders K. (2003) *Ap. J., 591,* 1220-1247. [27] Ray S. et al. (2020) *LPS LI,* Abstract #2558. [28] Ray S. et al. (2021) *In prep.* [29] McCoy T. J. and Bullock E. S. (2017) *Planetesimals,* 71-91. [30] Wilson L. and Keil K. (1991) *EPSL, 104,* 505-512. [31] Craddock P. R. et al. (2013) *EPSL, 365,* 63-76. [32] Savage P. S. and Moynier F. (2013) *EPSL, 361,* 487-496. [33] Fitoussi C. et al. (2009) *EPSL, 287,* 77-81. [34] Zambardi T. et al. (2013) *GCA, 121,* 67-83. [35] Fitoussi C. and Bourdon B. (2012) *Science, 335,* 1477-1480. [36] Chakrabarti R. and Jacobsen S. B. (2010) *GCA, 74,* 6921-6933. [37] Dauphas N. et al. (2015) *EPSL, 427,* 236-248. [38] Sikdar J. and Rai V. K. (2020) *Scientific Reports, 10,* 1273. [39] Pringle E. A. et al. (2014) *PNAS, 111*, 17029-17032. [40] Sossi P. A. et al. (2016) *EPSL, 449,* 360-371. [41] Hin R. C. et al. (2017) *Nature, 549,* 511-515. [42] Young E. D. et al. (2019) *Icarus, 323,* 1-15. [43] Poitrasson F. et al. (2019), *GCA, 267,* 257-274. [44] Savage P.S. et al. (2011) *GCA, 75,* 6124-6139. [45] Williams H. M. et al. (2006) *EPSL, 250,* 486-500. [46] Wang K. et al. (2012) *GCA, 89,* 31-45.